# Toward attosecond control of electron dynamics in two-dimensional materials

Mengxue Guan, Shiqi Hu, Hui Zhao, Chao Lian, and Sheng Meng

# Toward attosecond control of electron dynamics in two-dimensional materials Ⓕ

Mengxue Guan,[1,2] (iD) Shiqi Hu,[1,2] (iD) Hui Zhao,[1,2] Chao Lian,[1] (iD) and Sheng Meng[1,2,3,a] (iD)

**AFFILIATIONS**

[1]Beijing National Laboratory for Condensed Matter Physics and Institute of Physics, Chinese Academy of Sciences, Beijing 100190, China

[2]School of Physical Sciences, University of Chinese Academy of Sciences, Beijing 100190, China

[3]Songshan Lake Materials Laboratory, Dongguan, Guangdong 523808, China

[a]Author to whom correspondence should be addressed: smeng@iphy.ac.cn

**ABSTRACT**

Attosecond motion of strongly driven electrons encodes information on intense laser–solid interactions, leading to material- and laser-dependent photoemission and high-harmonic generation (HHG). Here, we investigate sub-cycle control over the electron dynamics in two-dimensional (2D) materials via adjusting the relative phase of two-color pulses. Electrons in 2D solids are sensitive to the exact shape of the optical field, showing properties similar to those of isolated atoms. Accompanied by spectra modulations, the resultant harmonic yields are enhanced and the cutoff energy increases to a ratio as large as 24% when an optimized phase is applied. Different from the atomic-like HHG, however, the cutoff energy is linearly dependent on the maximum strength of the light electric field, in line with that shown in conventional bulk solids. Thus, two-dimensional materials provide a unique platform where both bulk and atomic electron dynamics can be investigated. Our work suggests a simple way to generate optimized harmonic emission with existing experimental laser technology and offers a powerful tool for analyzing attosecond quantum dynamics during laser–solid interactions.

*Published under license by AIP Publishing.* https://doi.org/10.1063/1.5135599

Sub-cycle manipulation of electronic motion via intense laser pulses lies at the heart of attosecond science, allowing studies of ultrafast processes with unprecedented precision.[1–7] The resultant high-harmonic generation (HHG) can serve as a probe and provides insights into real-time electron dynamics in atoms, molecules, and solids.[6,8–12] Compared to the gas phases, laser–solid interactions are more complicated due to the diverse and complex electronic structures of solids. Thanks to the higher electronic density, solids not only provide another route toward compact and bright HHG sources[13] but also enable potential access to multi-petahertz electronics and all-optical processors.[14–16]

Among various condensed-matter systems, two-dimensional (2D) materials, such as graphene and monolayer transition-metal dichalcogenides, exhibit unique symmetries and electronic properties.[17–23] They provide a versatile platform to investigate the underlying electron processes, emerging as limiting cases of atomic-like and bulk-like dynamics. For instance, in monolayer hexagonal boron nitride, electrons exhibit similar real-space trajectories to those of the isolated atoms when the laser is perpendicular to the 2D plane, whereas normal bulk HHG response was found when electrons are driven in the plane of the monolayer.[24,25] Given all the interesting

equilibrium electronic properties and exotic optoelectronic applications envisioned, deep understanding and proper control of electron motions in 2D materials deserve much attention.

Here, we investigate, using the fully *ab initio* approach based on real-time time dependent density functional theory (rt-TDDFT), the sub-cycle electron dynamics in monolayer $MoS_2$ (1L-$MoS_2$) that is controlled via varying the relative phase of the two-color laser components, which have been widely used in gases,[26–29] plasma,[30,31] and bulk crystals.[32,33] We find a strong phase dependence of electron trajectories in momentum space, ascribed to the temporal variation of the incident field. The optimized phase is critical for the modulation of HHG spectrum morphology and the enhancement of harmonic yields. The cutoff energy is linearly dependent on the maximum strength of the laser pulse, which is consistent with HHG in bulk materials but in striking contrast to the quadratic dependence in atomic cases. Despite the discrepancies, the time-frequency analysis of HHG spectra shows that, similar to the atomic HHG, electron dynamics in 2D materials is sensitive to the interference between two pulses. Therefore, 2D materials provide a unique platform where both bulk-like and atomic-like responses can be achieved.

In our simulations, the laser electric field is described by a superposition of two monochromatic components linearly polarized along the zigzag direction of 1L-MoS$_2$, as shown in Fig. 1(a). The synthesized laser field can be expressed as
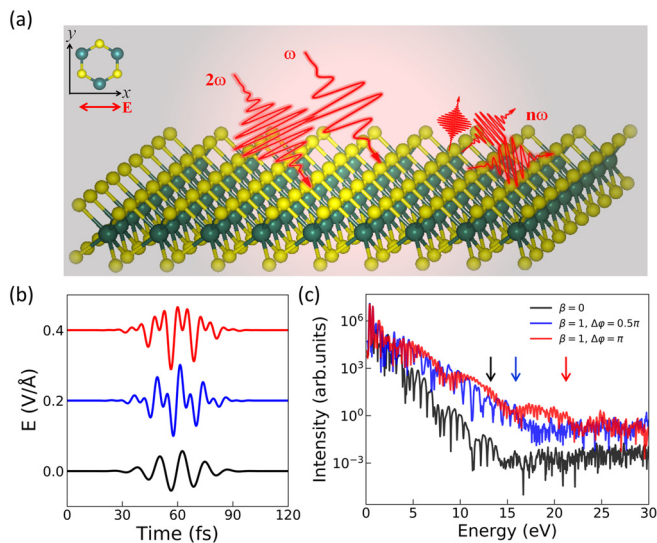
$$E(t) = E_0 f(t) \left[ \cos(\omega t) + \beta \cos(2\omega t + \Delta\varphi) \right]. \tag{1}$$

The pulse envelope $f(t)$ is defined as a Gaussian function,

$$f(t) = \exp\left[ -\frac{(t - t_0)^2}{2\sigma^2} \right]. \tag{2}$$

Herein, the width $\sigma$ is 12 fs and the photon energy of the fundamental field is set as $\hbar\omega = 0.32$ eV. The strength of the fundamental field is fixed and reaches the maximum $E_0 = 0.056$ V/Å (i.e., laser intensity $I = 0.09$ TW cm$^{-2}$) at time $t_0 = 60$ fs, while the ratio $\beta = E_2/E_1$ is a varying parameter and $\Delta\varphi$ defines the relative phase between the two pulses. For more calculation details, see the supplementary material, which involves Refs. 34–37.

Figure 1(c) shows HHG spectra generated in the three optical fields, which are displayed in Fig. 1(b): (i) the fundamental pulse only; the two-color pulses with the field-strength ratio $\beta$ fixed to 1 but with a relative phase, (ii) $\Delta\varphi = \pi$, or (iii) $\Delta\varphi = 0.5\pi$. It is clear that the participation of the frequency-doubled pulses leads to a significant extension of the cutoff photon energy, together with an enhancement of harmonic yields. Meanwhile, the shape of the spectra is sensitive to the relative phase between the two components. For $\Delta\varphi = 0.5\pi$, fairly discrete harmonic peaks can be observed with a single energy cutoff around 16 eV, while for $\Delta\varphi = \pi$, we can find a more continuous spectrum and two clear plateaus with a cutoff energy close to 14 and 22 eV, respectively. We focus on the second cutoff, whose energy is denoted
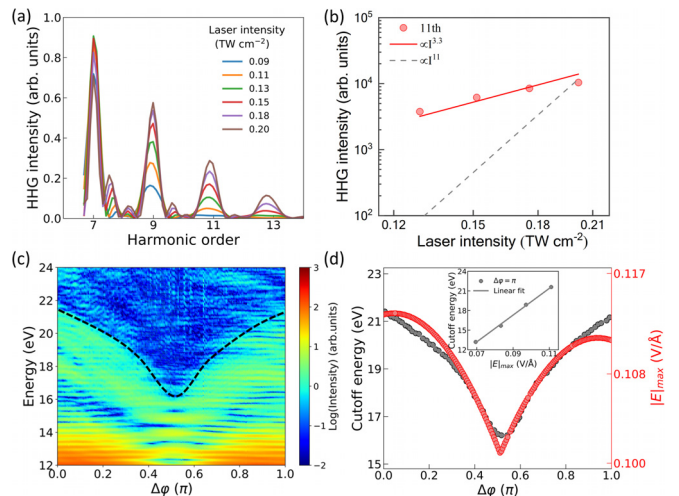
as $\varepsilon_c$. It is noteworthy to mention that because of the small gaps among conduction bands, the harmonic spectra do not show a sharp falling as that in gas phases, and therefore, the definition of cutoff energy is difficult. Here, we define that the cutoff is reached when $R_m = \frac{I_{m-2}}{I_m} \geq 10$, where $I_{m-2}$ and $I_m$ are the intensity of the $(m$-2)th and $m$th order harmonic emission, respectively.

Figure 2(a) shows the evolution of HHG spectra with the increase in laser intensity ($I$) under single-color pulses. The yield of the 11th-harmonic as a function of $I$ is displayed in Fig. 2(b), which scales as $I^{3.3}$, in good agreement with the previous experimental observation.[7] It shows the nonperturbative characteristic of the optoelectronic responses studied here since, in the perturbative regime, the $m$th harmonic yield is expected to scale as $I^m$.

Figure 2(c) summarizes the harmonic spectra as a function of $\Delta\varphi$ from 0 to $\pi$ when $\beta = 1$ (see Fig. S1 for the case with $\beta = 0.5$). A periodic and rather symmetric variation of $\varepsilon_c$ as a function of $\Delta\varphi$ is observed, and the maximum and minimum $\varepsilon_c$ values are found when $\Delta\varphi = 0$, $\pi$ and $\Delta\varphi = 0.5\pi$, accompanied by the synchronous enhancement or diminishment of harmonic yields. In this case, the modulation amplitude of $\varepsilon_c$, defined as $M = \frac{\max(\varepsilon_c) - \min(\varepsilon_c)}{\max(\varepsilon_c)}$, is about 24%.

Further studies reveal that the cutoff energy is closely related to the maximum module of electric field $|E|_{\max}$. In Fig. 2(d), the evolutions of $\varepsilon_c$ and $|E|_{\max}$ with $\Delta\varphi$ are displayed. It is obvious that two curves are in good agreement with each other, indicating that the sensitivity of cutoff energy in relative phase $\Delta\varphi$ results from the variation of $|E|_{\max}$. Taking into consideration that linear scaling on the vertical axes is used for two curves, it can be estimated that $\varepsilon_c \propto |E|_{\max}$, which is further confirmed by varying the intensity of the second pulse, i.e., the value of $\beta$ (Fig. S2). The inset shows the condition where $\beta$ increases from 0.25 to 1 in a step of 0.25 and $\Delta\varphi$ is set as $\pi$. The linear



**FIG. 1.** (a) Schematic illustration of 1L-MoS$_2$ illuminated by two-color pulses. The x and y axes are along the zigzag and armchair directions, respectively. In a typical experiment, the normal incidence two-color waveform is applied onto the monolayer and the emitted harmonics are detected in transmission. (b) Plot of the electric fields of the two-color pulses (red and blue) and fundamental only pulse (black), and the curves are shifted for clarity. (c) Corresponding HHG spectra. Vertical arrows mark the position of cutoff energies.



**FIG. 2.** (a) Dependence of HHG spectra on the fundamental laser intensity $I$. (b) The yield as a function of laser intensity of the 11th harmonic. (c) Calculated high-harmonic radiation as a function of relative phase between the two-color pulses. The black dashed line represents the estimated position of cutoff energy. (d) Evolution of cutoff energy (black dots) and $|E|_{\max}$ (red dots) as a function of $\Delta\varphi$. The inset shows the dependence of cutoff energy on $|E|_{\max}$ when the relative phase is fixed as $\Delta\varphi = \pi$.

scaling of $\varepsilon_c$ with $|E|_{max}$ from 1L-MoS$_2$ is consistent with the experimental observations on the HHG spectra produced in bulk solid materials such as ZnO and SiO$_2$,[6,38] but it is in striking contrast to the quadratic dependence for the cases of gas-phase atoms.[39]

We note that the deviations in the vicinity of 0 and $\pi$ might originate from the overestimation (or underestimation) of $\varepsilon_c$ due to the difficulty in obtaining their accurate values in the second plateau, where the adjacent orders have similar harmonic yields. Besides that, this discrepancy might be ascribed to some other mechanisms. For example, the electronic trajectories in the momentum, the electronic trajectories in the momentum space will influence the profile of the harmonic spectrum, and the slope of the linear relationship between $\varepsilon_c$ and $|E|_{max}$ might be changed accordingly. However, to fully resolve this open question, further investigations and analysis are needed.

The dynamics of harmonic generation is understood via performing time-frequency analysis.[40] As an example, we discuss the results of the relative phase $\Delta\varphi = 0.5\pi$ and $\Delta\varphi = \pi$, which are shown in Fig. 3, and there are some salient features. First, the lower-order harmonics are emitted at several instants during one optical cycle, while the highest harmonic radiations occur when the electric field reaches its extreme value. From the energy distribution, one can tell that it is $|E|_{max}$ that contributes to the higher cutoff energy of the spectrum. This suggests that the HHG cutoff can be controlled via the phase modulation, consistent with our observations discussed above.

Second, the participation of frequency-doubled pulses provides the possibility of sub-optical-cycle waveform control. As a result, either a smooth or a strongly modulated HHG spectrum is observed. For example, when $\Delta\varphi = 0.5\pi$, there are two adjacent main peaks with nearly the same intensity [labeled as A and B in Fig. 3(a)], leading to
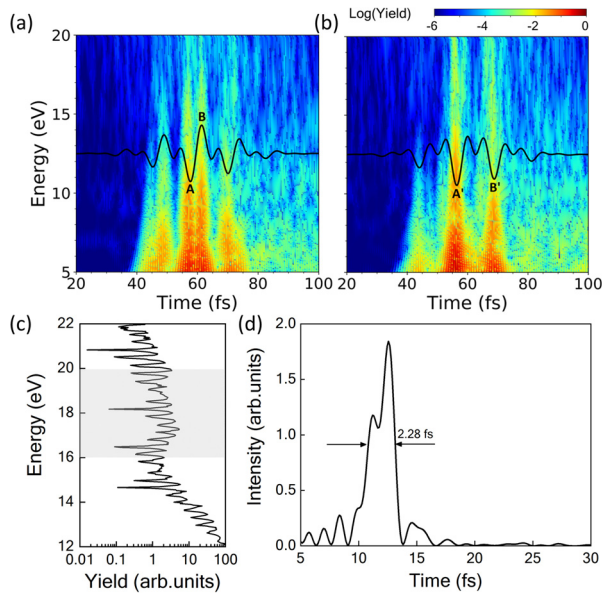


**FIG. 3.** Time-frequency analysis of the HHG spectra, two relative phase conditions are shown as examples: (a) $\Delta\varphi = 0.5\pi$ and (b) $\Delta\varphi = \pi$. The black line in each panel represents the corresponding electric field waveform. (c) Part of the HHG spectrum that is near the second plateau when $\Delta\varphi = \pi$. (d) The temporal profiles of the generated ultrashort pulse, which are obtained by performing inverse Fourier transformation of the shaded area in (c).

the generation of two extreme ultraviolet (EUV) bursts within half-cycle periodicity. Similar to the atomic phases,[27] the interference between the two bursts will produce fairly discrete harmonic peaks. However, when $\Delta\varphi = \pi$, the role of the frequency-doubled pulse is to enhance the amplitude difference between the central peak (A′) and the remaining peaks (e.g., B′) [Fig. 3(b)]. The single dominant EUV burst produces a more continuous spectrum.

These findings suggest that, in analogy to the generation of isolated attosecond EUV pulses via HHG in gases, a HHG spectrum, which has not only broad spectral width, but also a flat profile with least spectral modulation, can also be generated from 2D materials, permitting us to generate ultrashort pulses with a clean profile.[27,41] In this condition, by simply making an inverse Fourier transformation of the second plateau, the continuous spectrum can support a nearly isolated ultrashort pulse with a width of 2.28 fs at the energy in the EUV range ($\sim$20 eV) [Fig. 3(d)]. Comparable isolated EUV pulses, with a duration of 470 as, have been obtained in bulk SiO$_2$ by filtering the HHG spectra in the energy range of 18 eV–28 eV.[14] Note that the duration of the pulses, although being only half-cycle, is one order of magnitude longer than that generated from atomic gases ($\sim$100 as).[42] For generating ultrashort pulses with sub-100 as durations, EUV supercontinua with ultrabroad spectral widths ($\sim$60 eV) are required,[43] which might be accessed by further increasing the field amplitude. However, limited by the damage threshold, it is hard to achieve this target in solid materials at this stage. We note that even if the pulses generated are not sub-100-as in duration, they are still expected to find many interesting applications in time-resolved spectroscopy on solids on extreme time scales. The coherent EUV radiations that generated in solids are expected to advance laser photonics and electronics to a multi-petahertz frequency realm with great potential for scientific and technological inquiry, for example, tracing and attosecond control of strong-field electron dynamics.[15]

In order to obtain further insights into the underlying mechanisms of the phase modulation effect, we investigate the time-resolved electron distribution in the reciprocal space. In our previous works, we have demonstrated that the intraband dynamics play the dominant role in harmonic generation from 1L-MoS$_2$.[44] In this scenario, the validity of acceleration theorem is confirmed and the wave vector of the Bloch electron is thus linearly dependent on the vector potential of the laser pulse,[45,46]

$$k_A(t) = -\frac{e}{c\hbar}A(t) + k(t_0),\qquad(3)$$

where $t_0$ is the birth time of the electron wavepacket and

$$A(t) = -c\int_0^t E(t')dt'.\qquad(4)$$

Time evolutions of the module of vector potential $|A(t)|$ and the number of excited electrons $\Delta n\,(e^-)$ for $\Delta\varphi = 0.5\pi$ and $\Delta\varphi = \pi$ are shown in Figs. 4(a) and 4(b). It is clear that the oscillations of excited electrons are different from each other and both dependent on the respective $|A(t)|$. For $\Delta\varphi = 0.5\pi$, there is one prominent peak in the middle (A′) and two much lower peaks (one of them is labeled as B′) on both sides. In contrast, three peaks with similar strength appear when $\Delta\varphi = \pi$ and two of them are labeled as A and B.

In Figs. 4(c)–4(f), we show the details of the excited electron population at the moment of A and B for $\Delta\varphi = \pi$, as well as A′ and B′ for
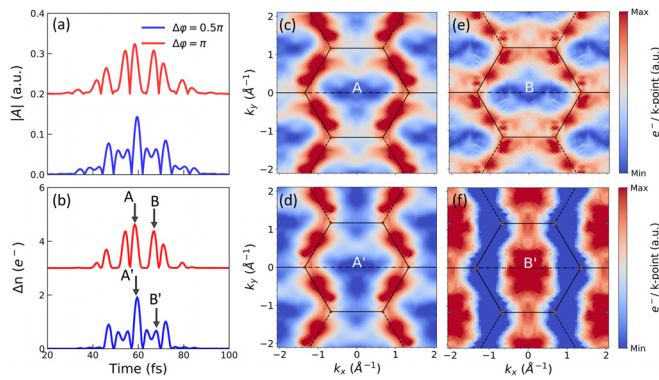
**FIG. 4.** (a) Time evolution of the module of vector potential and (b) the number of electrons excited to the conduction bands. In (a) and (b), the curves are shifted for clarity. (c)–(f) False color representation of the momentum space resolved distribution of the excited electrons at different moments in the relative phase $\Delta\varphi = \pi$ (c) and (e) and $\Delta\varphi = 0.5\pi$ (d) and (f).

$\Delta\varphi = 0.5\pi$. One can find that at A and A′, most of the electrons are excited to K and K′ valleys of the Brillouin zone (BZ) of 1L-MoS$_2$, indicating that electrons can be promoted to the same region of momentum space. However, when $\Delta n (e^-)$ reaches another peak, the distribution is reversed for $\Delta\varphi = 0.5\pi$ (i.e., B′) to the region along Γ-M, which is distinctly different from the condition for $\Delta\varphi = \pi$ (i.e., B). Therefore, the electron wave-packet may travel along the same trajectories in momentum space twice when $\Delta\varphi = \pi$, but only once for $\Delta\varphi = 0.5\pi$. This would generate much scattering at the boundary of BZ and thus higher yield of high-energy HHG in the former case.

We suggest that the above phenomena may explain qualitatively the appearance of the second plateau structure in the HHG spectrum. Until now, the two or multi-plateau structures have only been observed in experiment from rare-gas solids.[13] In many theoretical investigations, the multi-plateaus from the crystal have been predicted and are interpreted as a result of direct interband transitions involving high-lying bands.[47,48] Most recently, Li et al. demonstrated that in ZnO, the electrons located far from the top of the valence band (VB) can be accelerated to the top of the VB and contribute to the harmonics in the second plateau.[49] Our results suggest that the reciprocal-space trajectories of excited electrons play a dominant role in the emergence of the second plateau in the HHG spectrum, because comparable numbers of electrons are promoted to high-lying bands in both cases (Fig. S3), but electrons travel along different trajectories in the reciprocal space driven by phase modulations in the light electric field.

In conclusion, by using real time TDDFT, we have investigated sub-cycle control of electron motions in 1L-MoS$_2$ via applying two-color pulses. Our results show that the carrier wave-packet dynamics and the consequent harmonic emission are sensitive to the waveform of laser fields, which can be controlled by tuning the relative phase. As a result, the HHG cutoff energy can be extended, and the harmonic yields and spectrum profiles change accordingly. The obtained optimal spectrum ($\Delta\varphi = \pi$), accompanied by the second plateau structure, is a direct evidence of the potential to generate an isolated ultrashort pulse with a clean temporal profile from 2D materials. These findings have identified the similarities and discrepancies of electronic responses among 2D materials, isolated atoms, and bulk solids. Our results also open up opportunities for studying and ultimately controlling the ultrafast carrier dynamics and strong-field nonlinear behaviors in this type of material.

See the supplementary material for more discussions.

## REFERENCES

[1]M. Hohenleutner, F. Langer, O. Schubert, M. Knorr, U. Huttner, S. W. Koch, M. Kira, and R. Huber, Nature **523**, 572–575 (2015).
[2]T. Higuchi, C. Heide, K. Ullmann, H. B. Weber, and P. Hommelhoff, Nature **550**, 224 (2017).
[3]G. Vampa, T. J. Hammond, N. Thire, B. E. Schmidt, F. Legare, C. R. McDonald, T. Brabec, and P. B. Corkum, Nature **522**, 462–464 (2015).
[4]N. Tancogne-Dejean, O. D. Mucke, F. X. Kartner, and A. Rubio, Phys. Rev. Lett. **118**, 087403 (2017).
[5]O. Schubert, M. Hohenleutner, F. Langer, B. Urbanek, C. Lange, U. Huttner, D. Golde, T. Meier, M. Kira, S. W. Koch, and R. Huber, Nat. Photonics **8**, 119–123 (2014).
[6]S. Ghimire, A. D. DiChiara, E. Sistrunk, P. Agostini, L. F. DiMauro, and D. A. Reis, Nat. Phys. **7**, 138–141 (2011).
[7]H. Liu, Y. Li, Y. S. You, S. Ghimire, T. F. Heinz, and D. A. Reis, Nat. Phys. **13**, 262–265 (2017).
[8]J. Itatani, J. Levesque, D. Zeidler, H. Niikura, H. Pépin, J.-C. Kieffer, P. B. Corkum, and D. M. Villeneuve, Nature **432**, 867 (2004).
[9]T. Kanai, S. Minemoto, and H. Sakai, Nature **435**, 470 (2005).
[10]O. Smirnova, Y. Mairesse, S. Patchkovskii, N. Dudovich, D. Villeneuve, P. Corkum, and M. Y. Ivanov, Nature **460**, 972 (2009).
[11]H. B. Banks, Q. Wu, D. C. Valovcin, S. Mack, A. C. Gossard, L. Pfeiffer, R.-B. Liu, and M. S. Sherwin, Phys. Rev. X **7**, 041042 (2017).
[12]N. Tancogne-Dejean, O. D. Mucke, F. X. Kartner, and A. Rubio, Nat. Commun. **8**, 745 (2017).
[13]G. Ndabashimiye, S. Ghimire, M. Wu, D. A. Browne, K. J. Schafer, M. B. Gaarde, and D. A. Reis, Nature **534**, 520–523 (2016).
[14]M. Garg, M. Zhan, T. T. Luu, H. Lakhotia, T. Klostermann, A. Guggenmos, and E. Goulielmakis, Nature **538**, 359 (2016).
[15]F. Krausz and M. I. Stockman, Nat. Photonics **8**, 205 (2014).
[16]G. Vampa, T. J. Hammond, N. Thire, B. E. Schmidt, F. Legare, C. R. McDonald, T. Brabec, D. D. Klug, and P. B. Corkum, Phys. Rev. Lett. **115**, 193603 (2015).
[17]N. Kumar, S. Najmaei, Q. Cui, F. Ceballos, P. M. Ajayan, J. Lou, and H. Zhao, Phys. Rev. B **87**, 161403 (2013).
[18]R. Qin and Z.-Y. Chen, Nanoscale **10**, 22593–22600 (2018).
[19]Z.-Y. Chen and R. Qin, Nanoscale **11**, 16377–16383 (2019).
[20]T. Cao, G. Wang, W. Han, H. Ye, C. Zhu, J. Shi, Q. Niu, P. Tan, E. Wang, B. Liu, and J. Feng, Nat. Commun. **3**, 887 (2012).
[21]K. F. Mak, K. L. McGill, J. Park, and P. L. McEuen, Science **344**, 1489–1492 (2014).
[22]A. Chernikov, T. C. Berkelbach, H. M. Hill, A. Rigosi, Y. Li, O. B. Aslan, D. R. Reichman, M. S. Hybertsen, and T. F. Heinz, Phys. Rev. Lett. **113**, 076802 (2014).
[23]N. Yoshikawa, T. Tamaya, and K. Tanaka, Science **356**, 736–738 (2017).
[24]N. Tancogne-Dejean and A. Rubio, Sci. Adv. **4**, eaao5207 (2018).
[25]G. Le Breton, A. Rubio, and N. Tancogne-Dejean, Phys. Rev. B **98**, 165308 (2018).
[26]I. J. Kim, C. M. Kim, H. T. Kim, G. H. Lee, Y. S. Lee, J. Y. Park, D. J. Cho, and C. H. Nam, Phys. Rev. Lett. **94**, 243901 (2005).
[27]Z. Zeng, Y. Cheng, X. Song, R. Li, and Z. Xu, Phys. Rev. Lett. **98**, 203901 (2007).
[28]M. V. Frolov, N. L. Manakov, A. A. Silaev, and N. V. Vvedenskii, Phys. Rev. A **81**, 063407 (2010).

[29]D. Peng, L.-W. Pi, M. V. Frolov, and A. F. Starace, Phys. Rev. A **95**, 033413 (2017).

[30]M. R. Edwards, V. T. Platonenko, and J. M. Mikhailova, Opt. Lett. **39**, 6823–6826 (2014).

[31]M. Yeung, S. Rykovanov, J. Bierbach, L. Li, E. Eckner, S. Kuschel, A. Woldegeorgis, C. Rödel, A. Sävert, G. G. Paulus, M. Coughlan, B. Dromey, and M. Zepf, Nat. Photonics **11**, 32–35 (2017).

[32]J.-B. Li, X. Zhang, S.-J. Yue, H.-M. Wu, B.-T. Hu, and H.-C. Du, Opt. Express **25**, 18603 (2017).

[33]X. Liu, X. Zhu, P. Lan, X. Zhang, D. Wang, Q. Zhang, and P. Lu, Phys. Rev. A **95**, 063419 (2017).

[34]C. Lian, M. Guan, S. Hu, J. Zhang, and S. Meng, Adv. Theory Simul. **1**, 1800055 (2018).

[35]C. Lian, S.-Q. Hu, M.-X. Guan, and S. Meng, J. Chem. Phys. **149**, 154104 (2018).

[36]S. Meng and E. Kaxiras, J. Chem. Phys. **129**, 054110 (2008).

[37]K. F. Mak, C. Lee, J. Hone, J. Shan, and T. F. Heinz, Phys. Rev. Lett. **105**, 136805 (2010).

[38]T. T. Luu, M. Garg, S. Y. Kruchinin, A. Moulet, M. T. Hassan, and E. Goulielmakis, Nature **521**, 498–502 (2015).

[39]J. L. Krause, K. J. Schafer, and K. C. Kulander, Phys. Rev. Lett. **68**, 3535–3538 (1992).

[40]X.-M. Tong and S.-I. Chu, Phys. Rev. A **61**, 021802 (2000).

[41]O. D. Mücke, Phys. Rev. B **84**, 081202 (2011).

[42]T. Gaumnitz, A. Jain, Y. Pertot, M. Huppert, I. Jordan, F. Ardana-Lamas, and H. J. Wörner, Opt. Express **25**, 27506–27518 (2017).

[43]E. Goulielmakis, M. Schultze, M. Hofstetter, V. S. Yakovlev, J. Gagnon, M. Uiberacker, A. L. Aquila, E. Gullikson, D. T. Attwood, and R. Kienberger, Science **320**, 1614–1617 (2008).

[44]M.-X. Guan, C. Lian, S.-Q. Hu, H. Liu, S.-J. Zhang, J. Zhang, and S. Meng, Phys. Rev. B **99**, 184306 (2019).

[45]T.-Y. Du and X.-B. Bian, Opt. Express **25**, 151–158 (2017).

[46]S. Y. Kruchinin, F. Krausz, and V. S. Yakovlev, Rev. Mod. Phys. **90**, 021002 (2018).

[47]X. Liu, X. Zhu, X. Zhang, D. Wang, P. Lan, and P. Lu, Opt. Express **25**, 29216–29224 (2017).

[48]M. Wu, S. Ghimire, D. A. Reis, K. J. Schafer, and M. B. Gaarde, Phys. Rev. A **91**, 043839 (2015).

[49]L. Li, P. Lan, X. Zhu, T. Huang, Q. Zhang, M. Lein, and P. Lu, Phys. Rev. Lett **122**, 193901 (2019).